



**16th  
SYMPOSIUM  
OF THE IAHR**

SECTION ON HYDRAULIC MACHINERY  
AND CAVITATION  
SÃO PAULO / BRAZIL

16th to 19th SEPTEMBER 1997



**HYDRAULIC ANALYSIS OF FLOW  
COMPUTATION RESULTS**

**ANALYSE HYDRAULIQUE DES RESULTATS  
DE CALCUL D'ECOLEMENT**

Olivier SANTAL

Ecole Polytechnique Fédérale de Lausanne

Switzerland

33, Avenue de Cour

1007 Lausanne

Switzerland

François AVELLAN

Ecole Polytechnique Fédérale de Lausanne

Switzerland

**SUMMARY**

To get rid of all numerical aspects in flow simulation results and to have more informations about the evolution of the physical values inside the computational domain, we have developed a controlling and analysing method of these results. This method is based on the physical conservation laws. The balances are computed on the external surfaces of the computational domain and on a liquid surface moving along the main flow direction. The use of this method is illustrated in the case of an Euler code. This method allowed us to correct this Euler code and to define a domain of validity for the numerical results obtained.

**RESUME**

Pour se départir des problèmes liés à l'aspect numérique d'un résultat de calcul et pour avoir plus d'informations sur l'évolution des grandeurs physiques à l'intérieur du domaine de calcul, nous avons développé une méthode de contrôle et d'analyse de ces résultats. La méthode est basée sur les équations de conservation des grandeurs physiques. Les bilans sont calculés sur les surfaces extérieures au domaine de calcul et sur une surface liquide se déplaçant suivant la direction principale de l'écoulement. L'utilisation de cette méthode de contrôle est démontrée dans le cas d'un code Euler. Elle nous a permis de corriger ce code Euler et de définir un domaine de validité des résultats numériques obtenus.

## INTRODUCTION

In the flow simulation, the first classical action one does, is the verification of the convergence of numerical results by watching the evolution of velocity, pressure or other residues as a function of iteration number. If these residues reach the convergence criteria defined by the user, according to the computer case, then the solution is said to be numerically converged. But we still have to know whether these results are physically meaningful, since, due to numerical approximations implemented in the code ( modelization, discretization, simplification ... ) some discrepancies may appear between the computed values and the reality.

Until now two different methods were usable to analyse the results :

- the computation of global physical values as : flow rate at the inlet and outlet, torque or forces on the blades, ...
- the visualization of the flow or pressure fields.

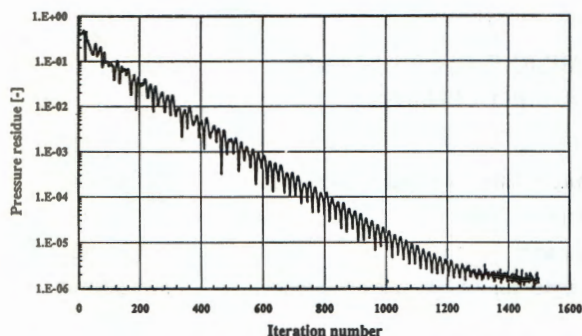


Figure 1 Typical convergence curve as pressure residues function of iteration number

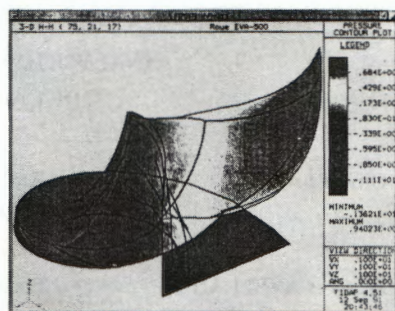


Figure 2 Visualization of the pressure field in a Francis runner

The first method is very interesting in order to have the balance of physical fluxes between the surfaces surrounding the computational domain, yet this method is unable to provide any information on the evolution of these fluxes inside the domain. For example, if the flow rate at the inlet is not the same as the one at the outlet, we can not conclude whether it is due to a discontinuity of the mesh, or to a numerical evolution.

The second method is only valid when you are sure of the results, to see the local variations of the values, or to compute other derived values as streamlines. But, it will be inefficient for showing a flow mass discontinuity, as for example, the evolution of the energy transfer along a runner blade, or the evolution of the drag along a wing.

For all these reasons, we have developed a method to evaluate numerical results by the use of simple physical conservation laws of hydraulic in an intrinsic manner.

## PRINCIPLES

The IMHEF Euler code will be considered in this paper to detailed our method of flux control. This code allows us to compute incompressible, inviscid and steady-state flows in a stationary or rotating frame of reference. It has the following numerical features : structured meshes, a finite volume discretization scheme, a three steps Runge-Kutta resolution scheme, a pseudo compressibility scheme to compute the pressure and a pseudo viscosity scheme for the dissipation [1][2][3]. We also take H-H mesh types which are quite well adapted to the computation of hydraulic machinery [4]. The basic idea of the method of flux control is to survey, along any specific mesh lines, the evolution of the flow rate, momentum, moment of momentum and energy fluxes on mesh faces. When using an Euler code, the fluxes computed by our method will be : flow rate, momentum in the case of stationary elements (stay-vanes, guide-vanes, ... ) or moment of momentum for the rotating parts (runner) and the energy. The latest one is computed even in the case of Euler code in order to see the energy coupling between kinetic terms and pressure. When we compute the momentum or the moment of momentum we split the computational domain in two parts :

- liquid faces : which include the inlet, the outlet and the faces going from the inlet to the outlet along a specific logical line,
- the other faces, among which the walls.

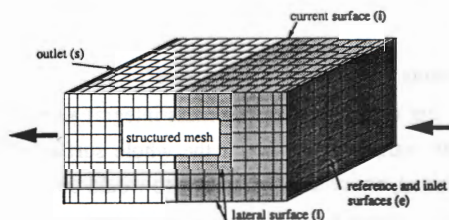


Figure 3 Schematic drawing of a H-H mesh, with definition of mesh faces

The interest of this partition is to distinguish what is supplied to the system by the fluid, from what is transformed or restored by the system along the walls (blades), in terms of forces for stationary parts and in terms of torque in a rotating case.

When a H-H type mesh is used, the specific mesh line taken is easily found, as it is the median logical mesh line corresponding of the dominating convection flow.

To compute the fluxes, we use the following integrals :

- flow rate :

$$\int_{A_e} \vec{c} \cdot \vec{n} dA = - \int_{A_{s+1}} \vec{c} \cdot \vec{n} dA \quad (1)$$



- momentum for stationary parts :

$$\int_A \vec{c} [\vec{c} \cdot \vec{n}] dA + \int_{A_{e+s}} \left[ \frac{\vec{p}}{\rho} + \vec{g} \cdot \vec{r} \right] \vec{n} dA = - \int_{A_I} \left[ \frac{\vec{p}}{\rho} + \vec{g} \cdot \vec{r} \right] \vec{n} dA + \varepsilon_m \quad (2)$$

- moment of momentum for rotating parts :

$$\begin{aligned} \int_A \left[ \vec{r} \times \vec{w} \right] \vec{w} \cdot \vec{n} dA + \int_{A_{e+s}} \vec{r} \times \left[ \frac{\vec{p}}{\rho} + \vec{g} \cdot \vec{r} \right] \vec{n} dA + \int_V \left[ \vec{\omega} \times \vec{\omega} \times \vec{r} + 2 \vec{\omega} \times \vec{w} \right] dV \\ = - \int_{A_I} \vec{r} \times \left[ \frac{\vec{p}}{\rho} + \vec{g} \cdot \vec{r} \right] \vec{n} dA + \varepsilon_{mm} \end{aligned} \quad (3)$$

- power or energy flux :

$$\int_A \left[ \frac{\vec{p}}{\rho} + \frac{1}{2} \vec{c}^2 + \vec{g} \cdot \vec{r} \right] \vec{c} \cdot \vec{n} dA = \varepsilon_e \text{ or } \int_A \left[ \frac{\vec{p}}{\rho} + \frac{1}{2} \vec{w}^2 - \frac{1}{2} [\vec{\omega} \times \vec{r}]^2 + \vec{g} \cdot \vec{r} \right] \vec{w} \cdot \vec{n} dA = \varepsilon_e \quad (4)$$

With the following remarks :

- the symbol  $\varepsilon$  means : "global numerical losses",
- the partition of the surface in the flow mass integral allows the visualization of the evolution of this value. Otherwise, if the whole surface is taken into account to compute the integral, a resulting flux near zero would be obtained.

With this Euler code, the above integrals have the following meaning :

- flow rate : checks if the velocity field computed with the momentum equations verifies the mass conservation equation, thereby controlling that the pseudo compressibility scheme does not create any artificial source,
- momentum or moment of momentum : the fluxes show the energetic transfer between velocity and pressure,
- energy : the flux shows the effect of the pseudo viscosity scheme. The coupling of the velocity and the pressure is also illustrated in terms of total energy, since the mass conservation and momentum equations are the only ones used to compute velocity and pressure fields.

In order to avoid any artificial discrepancy between the results and the analysis, identical discretization schemes between the controlled and the controlling codes must be used for integrating the fluxes. To each type of code will correspond a specific controlling software.

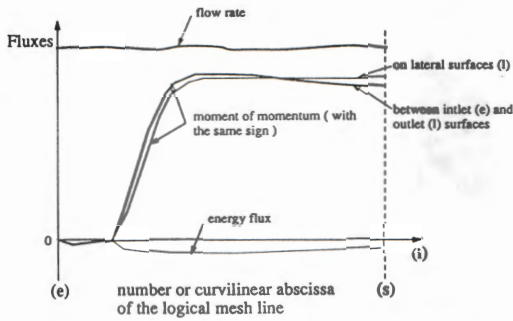


Figure 4 Typical flux control curves in an hydraulic runner

The values of fluxes are then represented as a function of the logical position or of the curvilinear abscissa on the mesh line, since each mesh line in a structured mesh can be described by a sole index. The integrated values on liquid faces are shown with the same sign as the ones on walls, equations (2) or (3) ; thus it makes it possible to directly compare these two fluxes.

#### IMPLEMENTATION IN THE EULER CODE

The computation of the elementary fluxes on a face between two contiguous cells in the IMHEF Euler code is done by performing the arithmetic mean of the local velocity components and of the pressure according to the following :

- flow rate

$$\Delta q = \frac{1}{2} \left[ \vec{c}_1 + \vec{c}_2 \right] \cdot \vec{dA} \quad (5)$$

- momentum

$$\frac{1}{2} \left[ \left[ \vec{c}_1 \cdot \vec{dA} \right] \vec{c}_1 + \left[ \vec{c}_2 \cdot \vec{dA} \right] \vec{c}_2 \right] + \frac{1}{2} \left[ \frac{p_1 + p_2}{\rho} + \vec{g} \cdot \left[ \vec{r}_1 + \vec{r}_2 \right] \right] \vec{dA} \quad (6)$$

The elementary moment of momentum flux is done in a similar way ( as this value is not calculated in the Euler code ).

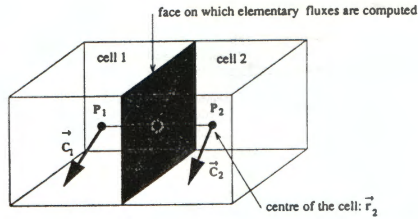


Figure 5 Schematic drawing of mesh face with contiguous cells

moment of momentum

$$\frac{1}{4} \left[ \left[ \vec{c}_1 \cdot d\vec{A} \right] \vec{c}_1 + \left[ \vec{c}_2 \cdot d\vec{A} \right] \vec{c}_2 \right] \times (\vec{r}_1 + \vec{r}_2) +$$

$$\frac{1}{4} \left[ \frac{\vec{p}_1 + \vec{p}_2}{\rho} + \vec{g} \cdot (\vec{r}_1 + \vec{r}_2) \right] \left[ d\vec{A} \times (\vec{r}_1 + \vec{r}_2) \right] \quad (7)$$

energy

$$\frac{1}{2} \left[ \left[ \frac{\vec{p}_1}{\rho} + \frac{1}{2} \vec{c}_1^2 + \vec{g} \cdot \vec{r}_1 \right] \vec{c}_1 + \left[ \frac{\vec{p}_2}{\rho} + \frac{1}{2} \vec{c}_2^2 + \vec{g} \cdot \vec{r}_2 \right] \vec{c}_2 \right] \cdot d\vec{A} \quad (8)$$

A similar discretization is used for the rotating flow.

The next step is to sum up all these elementary fluxes on each different surfaces of the domain : inlet, lateral faces including walls, periodic boundaries, ... and internal surface at a given position along the previously defined mesh line. The last step is to move this position from the inlet to the outlet in order to obtain a complete survey of the fluxes inside the domain. For instance, the following function is obtained for the mass conservation equation :

$$Q(i) = \sum_{(i)=(e)}^{(i)=(s)} \sum_{A_{i+1}} \Delta q \quad (9)$$

Where  $i$  is the index of the median mesh line,  $\Delta q$  the elementary quantity defined in equation (5) and  $Q$  the flow rate.

## IMPLEMENTATION IN THE CASE OF A NAVIER-STOKES CODE

We can expand this method to the case of finite element Navier-Stokes code. This demonstration is illustrated with the general purpose finite element program FIDAP of Fluid Dynamics International, Inc. . In this case the equation are different since it is necessary to introduce the Reynolds stress tensor. The corresponding integrals are written :

- flow mass : identical to the Euler case,
- momentum for stationary parts :

$$\int_A \left[ \vec{c} \left[ \vec{c} \cdot \vec{n} \right] + \frac{\vec{\tau}}{\rho} \cdot \vec{n} \right] dA + \int_{A_{e+s}} \left[ \frac{\vec{p}}{\rho} + \vec{g} \cdot \vec{r} \right] \vec{n} dA = - \int_{A_I} \left[ \frac{\vec{p}}{\rho} + \vec{g} \cdot \vec{r} \right] \vec{n} dA \quad (10)$$

- moment of momentum for rotating parts :

$$\int_A \vec{r} \times \left[ \vec{w} \left[ \vec{w} \cdot \vec{n} \right] + \frac{\vec{\tau}}{\rho} \cdot \vec{n} \right] dA + \int_{A_{e+I}} \vec{r} \times \left[ \frac{\vec{p}}{\rho} + \vec{g} \cdot \vec{r} \right] \vec{n} dA + \int_V \left[ \vec{\omega} \times \vec{\omega} \times \vec{r} + 2 \vec{\omega} \times \vec{w} \right] dV = - \int_{A_I} \vec{r} \times \left[ \frac{\vec{p}}{\rho} + \vec{g} \cdot \vec{r} \right] \vec{n} dA \quad (11)$$

- power or energy flux :

$$\int_A \left[ \frac{1}{2} \vec{c}^2 + \vec{g} \cdot \vec{r} \right] \vec{c} \cdot \vec{n} dA + \int_A \left[ \vec{n} \left[ \frac{\vec{p}}{\rho} \vec{I} + \frac{\vec{\tau}}{\rho} \right] \right] \cdot \vec{c} dA = 0 \quad (12)$$

As we said before, we have to take into account the scheme used in this specific code that is to say the discretization of the equations in terms of basic functions. Since our geometries are treated with structured meshes of eight node isoparametric bricks as elements, we use a decomposition in trilinear interpolation functions to compute the surface and volume integrals.

$$\int_{-1}^1 \int_{-1}^1 \vec{q} \cdot \vec{n} J dr du \quad \text{or} \quad \int_{-1}^1 \int_{-1}^1 \int_{-1}^1 \vec{q} J dr du dv \quad (13)$$

where  $\vec{q}$  is one of the computed value defined in equations (1), (10), (11) or (12) and  $J$  the jacobian of the geometrical transform.

These integrals of elementary fluxes are calculated either in an analytic way or by using a gaussian quadrature. Finally, the same summation as described in formulation (9) is used with the values defined in equations (13).

## EXAMPLES OF APPLICATION

To illustrate the method, we present two examples from our experience in the use of our Euler code. The first example illustrates an interesting result of this control procedure, as it enabled us to correct our numerical discretization scheme. The second example shows how to avoid any disturbance generated by the outlet boundary condition.

### Modification of the discretization scheme

Computations with the Euler code were performed in a Francis runner geometry, and the following results were obtained :

- a very good numerical convergence ( up to  $10^{-5}$  in term of pressure residue ),
- a discrepancy between the inlet and the outlet mass flow of 1.4 %,
- a torque integrated on the blades 17.8 % greater then the balance of moment of momentum between the inlet and the outlet of the computational domain.

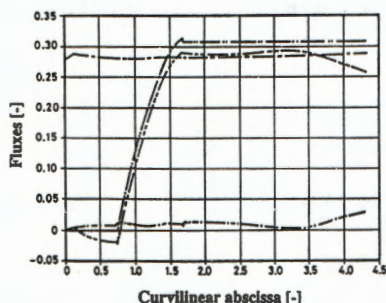


Figure 6 Flux control before correction

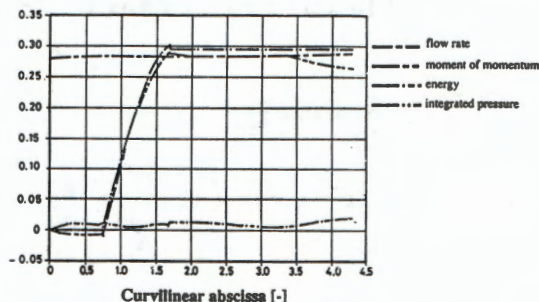


Figure 7 Flux control after correction

The latest result is totally unacceptable, because it shows an internal production of hydraulic energy and therefore modifies the initial operating point.

After checking all the different aspects of the numerical parameters such as for example the size of mesh cells near the blades or the extrapolation of the pressure on the blades we found it impossible to explain this production of energy. Even 3-D colour images of velocity or pressure fields seemed to be correct. Fortunately experimental values of the averaged velocity and pressure at the inlet and outlet as well as the pressure field on the blades were available to compare them with the flow



computation. Yet the small differences between experimental [5] and computed [6] values were not sufficient to explain the increase of torque.

The fluxes gave more information about the evolution of the torque and the moment of momentum, as they emphasized a discontinuity of flow rate and moment of momentum just after the inlet boundary condition. This information was self-important enough to determine the numerical problem causing the discontinuity and to enable its solving.

### Truncation of the computed domain

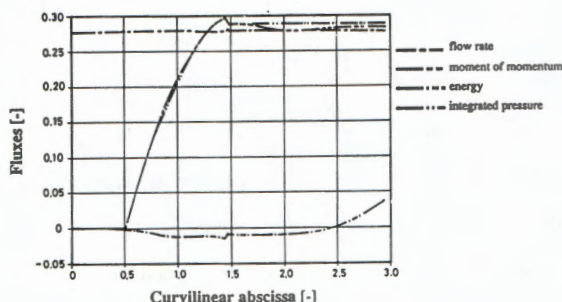


Figure 8 Truncated domain where the conservation laws are checked

Analysing the previous results one can observe near the outlet boundary surface local variations moment of momentum. The global results of the torque and the moment of momentum show same behaviour, even with the previous correction done. Using the flux analysis, we are able to determine the domain where the decrease of moment of momentum occurs. Since this sub-domain begins a few cells after the trailing edge and continues up to the outlet, we can assume results inside the runner are correct and remove this sub-domain from the control domain for global analysis. Doing so we can keep the numerical results even with though it shows a numerical problem at the outlet boundary, since this problem is probably a reflecting boundary condition which will take time to correct.

### CONCLUSIONS

To have more information than only convergence curve and coloured images of velocity or pressure fields, we have developed a method which allows to control and also analyse all the physical evolutions of flow simulation results inside hydraulic machinery. This method also helps the understanding of the numerical behaviour of computational codes in a physical way. As a result it eased the improvement of the numerical shape of our Euler code and it helps to determine a domain of validity of the computed results. This tool is now a full part of our analysis process.

## ACKNOWLEDGMENTS

The authors wish to acknowledge the contribution made by their colleagues from the IMHEF Evaluation of Performances Research Group. This work is financially supported by the Sulzer Escher Wyss company and the Hydro Vevey company.

## LIST OF SYMBOLS

$\vec{c}$	Absolute velocity	[m s <sup>-1</sup> ]	$\vec{w}$	Relative velocity	[m s <sup>-1</sup> ]
$p$	Static pressure	[Pa]	$\rho$	Density	[kg m <sup>-3</sup> ]
$\vec{g}$	Gravity acceleration	[m s <sup>-2</sup> ]	$\vec{r}$	Vector	[m]
$\vec{\omega}$	Rotating speed	[rad s <sup>-1</sup> ]	$t$	Time	[s]
$\vec{n}$	Normal unity vector	[-]	$dA$	Elementary surface	[m <sup>2</sup> ]
$dV$	Elementary volume	[m <sup>3</sup> ]	$J$	Jacobian	[m <sup>3</sup> ]
$\tau$	Reynolds stress tensor	[Pa]	$\bar{I}$	Identity tensor	[-]
$r, u, v$	Intrinsic variables	[-]			

For the indices we have: e : inlet, s : outlet, l : lateral surfaces.

## REFERENCES

- [1] L.E Eriksson, A. Rizzi, J.P. Therre, *Numerical solution of steady incompressible Euler equations applied to water turbines* AIAA-84-2145 .
- [2] E. Goede, R. Cuenod, P. Bachmann, *Theoretical and experimental investigation of the flow field around a Francis runner*, IAHR-AIRH symposium 1988 Trondheim.
- [3] F. Thibaud, A. Drotz, G. Sottas, *Validation of an Euler code for hydraulic turbines* AGARD symposium, Lisbon, Portugal; May 1988.
- [4] C. Neury, A. Bottaro, *Influence de la topologie du maillage dans la simulation des machines hydrauliques*, rapport IMHEF/EPFL1990.
- [5] *Proceedings of the GAMM Workshop*, 1989, Lausanne, to be published by Vieweg Verlag in the series *Notes on Numerical Fluid Mechanics* .
- [6] F. Avellan, P. Dupont, M. Farhat, B. Gindroz, P. Henry, M. Hussain, E. Parkinson, O. Santal, *Flow survey and blade pressure measurements in a Francis turbine model*, IAHR symposium, Belgrade (1990) .